Transport measurement of the orbital Kondo effect with ultracold atoms

Yusuke Nishida

Department of Physics, Tokyo Institute of Technology, Ookayama, Meguro, Tokyo 152-8551, Japan

(Dated: August 2015)

The Kondo effect in condensed-matter systems manifests itself most sharply in their transport measurements. Here we propose an analogous transport signature of the orbital Kondo effect realized with ultracold atoms. Our system consists of imbalanced Fermi seas of two components of fermions and an impurity atom of different species which is confined by an isotropic potential. We first apply a $\pi/2$ pulse to transform two components of fermions into two superposition states. Their interactions with the impurity atom then cause a "transport" of fermions from majority to minority superposition states, whose numbers can be measured after applying another $3\pi/2$ pulse. In particular, when the interaction of one component of fermions with the impurity atom is tuned close to a confinement-induced p-wave or higher partial-wave resonance, the resulting conductance is shown to exhibit the Kondo signature, i.e., universal logarithmic growth by lowering the temperature. The proposed transport measurement will thus provide a clear evidence of the orbital Kondo effect accessible in ultracold atom experiments and pave the way for developing new insights into Kondo physics.

I. INTRODUCTION

The Anderson impurity model is one of the most important and fundamental model Hamiltonians in condensed-matter physics [1]. It was originally invented to study localized magnetic impurities in metallic environments and there exist three distinct parameter regimes called empty orbital regime, mixed valence regime, and local moment regime [2]. Of particular interest is the local moment regime, where the electrical resistivity grows logarithmically toward the low temperature as a consequence of the celebrated Kondo effect [3, 4]. By extending the Anderson impurity model, orbital degeneracy can also be incorporated [5] and periodic arrangement of magnetic impurities is considered to be relevant to heavy fermion physics [6].

Further application of the Anderson impurity model is possible by introducing additional degrees of freedom corresponding to left and right leads to study tunneling of electrons through a quantum dot both in and out of equilibrium [7, 8]. In fact, one degree of freedom can be decoupled by a canonical transformation and the other interacting degree of freedom turns out to be described by the original Anderson impurity model [9]. Therefore, the Kondo effect emerges again in quantum dot systems but now as the logarithmic growth of the electrical conductance by lowering the temperature [9, 10], where a number of beautiful observations of the Kondo effect have been made [11, 12].

The purpose of this Rapid Communication is to show that all the rich physics associated with the Anderson impurity model can be simulated with ultracold atoms by employing standard techniques such as magnetic-field-induced Feshbach resonances, species-selective optical lattices, and laser couplings of atomic hyperfine states [13]. In particular, we place special emphasis on the transport measurement of the Kondo effect analogous to quantum dot experiments, which should be of great importance in ultracold atom experiments because transport is usually difficult to study with the exception of recent progress made in Refs. [14–20]. Future realization of the Kondo effect and its transport measurement with ultracold atoms will pave the way for developing new insights into yet unresolved aspects of Kondo physics such as the formation and dynamics of the Kondo screening cloud [21] and the quantum criticality in heavy fermion systems [6].

II. SETUP AND MEASUREMENT PROTOCOL

Our study is based on the simple and versatile scheme to realize the orbital Kondo effect with ultracold atoms [22] (see Refs. [23–33] for other proposals). The system consists of a Fermi sea of spin-polarized $\uparrow$ fermions of species A interacting with a spinless impurity atom of different species B which is loaded into a ground state of an isotropic potential. By tuning the interspecies attraction with an s-wave Feshbach resonance, the impurity atom and a spin-polarized fermion can form a bound molecule that occupies a degenerate orbital of the confinement potential with orbital angular momentum $\ell \geq 1$ [34]. In particular, when the total energy of the bound molecule coincides with the scattering threshold of the $A_\uparrow$ and B atoms, an ℓth partial-wave resonance is induced and low-energy physics in its vicinity is described by a two-channel Hamiltonian:

$$H_\uparrow = \int \frac{d\boldsymbol{k}}{(2\pi)^3}\, \epsilon_{\boldsymbol{k}}\, \psi_{A\uparrow}^\dagger(\boldsymbol{k})\psi_{A\uparrow}(\boldsymbol{k}) + \sum_{m=-\ell}^{\ell} \delta_m \phi_m^\dagger \phi_m$$
$$+ \sum_{m=-\ell}^{\ell} \int \frac{d\boldsymbol{k}}{(2\pi)^3} \left[V_\ell^m(\boldsymbol{k}) \psi_{A\uparrow}^\dagger(\boldsymbol{k}) \psi_B^\dagger \phi_m + \text{H.c.} \right]. \quad (1)$$

Here $\psi_{A\uparrow}^\dagger(\boldsymbol{k})$ creates an $A_\uparrow$ atom with energy $\epsilon_{\boldsymbol{k}} = \hbar^2 \boldsymbol{k}^2/(2M)$, while $\psi_B^\dagger$ creates the impurity B atom in

the ground state of the confinement potential whose energy is chosen to be zero. The bound molecule is created by $\phi_m^\dagger$ in one of the degenerate orbitals labeled by the magnetic quantum number $|m| \leq \ell$. Its coupling to the $A_\uparrow$ and B atoms is assumed to have the harmonic form of

$$V_\ell^m(\boldsymbol{k}) = v_m |\boldsymbol{k}|^\ell Y_\ell^m(\hat{\boldsymbol{k}}) \exp\left[-\frac{\boldsymbol{k}^2}{2\Lambda^2}\right] \qquad (2)$$

with the wave-number cutoff Λ set by an inverse characteristic extent of the confined B atom. Because only one B atom is confined, the particle number operators of the localized B atom and bound molecule are constrained by

$$N_B = \psi_B^\dagger \psi_B + \sum_{m=-\ell}^{\ell} \phi_m^\dagger \phi_m = 1. \qquad (3)$$

When the rotational symmetry is exact, we have an equal detuning δ_m and coupling v_m for all m and thus the degeneracy is $(2\ell+1)$-fold, while we shall develop a general formulation so that it is also applicable to study the effect of symmetry breaking later.

Interestingly, the low-energy effective Hamiltonian (1) naturally realizable with ultracold atoms is nothing but the infinite-U Anderson impurity model in the slave-particle representation [35, 36] with its fictitious degrees of freedom corresponding to our real atom and molecule as in Eq. (3). The empty orbital, mixed valence, and local moment regimes of the original Anderson impurity model are thus translated into atomic regime ($\langle \psi_B^\dagger \psi_B \rangle \simeq 1$), resonant regime ($0 \lesssim \langle \psi_B^\dagger \psi_B \rangle \lesssim 1$), and molecular regime ($\langle \psi_B^\dagger \psi_B \rangle \simeq 0$), respectively, in the language of ultracold atoms. In particular, the orbital Kondo effect emergent in the molecular limit was elaborated for $\ell = 1$ in Ref. [22], while the analysis therein can be straightforwardly generalized for an arbitrary ℓ to find that the Kondo temperature in the SU($2\ell+1$) symmetric case has a universal leading exponent given by

$$T_\mathrm{K} \propto T_\mathrm{F} \exp\left[-\frac{\pi}{(2\ell+1)a_\ell k_\mathrm{F}^{2\ell+1}}\right] \qquad (4)$$

with $a_\ell \ll k_\mathrm{F}^{-2\ell-1}$ being the ℓth partial-wave scattering length. Because the Kondo effect in condensed-matter systems manifests itself most sharply in their transport measurements, it is highly desired although challenging to establish an analogous transport signature of the orbital Kondo effect in ultracold atom experiments.

In what follows, we indeed show that the conductance measurement of the Kondo effect in quantum dot experiments can be equivalently performed with ultracold atoms by adopting the idea from Ref. [37]. To this end, we introduce another spin $\downarrow$ component of fermionic species A,

$$H_\downarrow = \int \frac{d\boldsymbol{k}}{(2\pi)^3} \, \epsilon_{\boldsymbol{k}} \, \psi_{A\downarrow}^\dagger(\boldsymbol{k}) \psi_{A\downarrow}(\boldsymbol{k}), \qquad (5)$$

as well as the intercomponent coupling driven by a resonant laser field with the Rabi frequency Ω,

$$H_{\uparrow\downarrow} = i\frac{\hbar\Omega}{2} \int \frac{d\boldsymbol{k}}{(2\pi)^3} \left[\psi_{A\uparrow}^\dagger(\boldsymbol{k})\psi_{A\downarrow}(\boldsymbol{k}) - \psi_{A\downarrow}^\dagger(\boldsymbol{k})\psi_{A\uparrow}(\boldsymbol{k})\right], \qquad (6)$$

which are expressed in the rotating frame. It is legitimate to assume that interactions of $A_\downarrow$ atoms with $A_\uparrow$ atoms and with the impurity B atom are both negligible in the dilute limit because they are generally off-resonance when the interaction of $A_\uparrow$ atoms with the impurity B atom is tuned close to a confinement-induced resonance. It is also important that the confinement-induced resonance can be turned on and off without changing the magnetic field but by controlling the potential strength acting on the impurity B atom [34]. With all these setups, we are ready to propose a simple conductance measurement with ultracold atoms consisting of the following three protocols.

(i) Preparation: We first stay away from any confinement-induced resonances so that both $A_\uparrow$ and $A_\downarrow$ atoms negligibly interact with the impurity B atom. After introducing N_- and N_+ numbers of $A_\uparrow$ and $A_\downarrow$ atoms, we apply the intercomponent coupling (6) for a duration of $\pi/(2\Omega)$, which transforms the two spin components into two superposition states according to $|A_\uparrow\rangle \to |A_-\rangle \equiv (|A_\uparrow\rangle - |A_\downarrow\rangle)/\sqrt{2}$ and $|A_\downarrow\rangle \to |A_+\rangle \equiv (|A_\uparrow\rangle + |A_\downarrow\rangle)/\sqrt{2}$. Consequently, N_- and N_+ numbers of A_- and A_+ atoms are prepared at a common temperature T and their corresponding chemical potentials are denoted by $\mu_- \equiv \mu - \Delta\mu/2$ and $\mu_+ \equiv \mu + \Delta\mu/2$, respectively.

(ii) Transport: We now turn on the confinement-induced ℓth partial-wave resonance of $A_\uparrow$ atoms with the impurity B atom. Because A atoms are prepared on the $\pm$ basis, it is appropriate to express the total Hamiltonian composed of Eqs. (1) and (5) in terms of the corresponding creation operators $\psi_{A\pm}^\dagger(\boldsymbol{k}) \equiv [\psi_{A\uparrow}^\dagger(\boldsymbol{k}) \pm \psi_{A\downarrow}^\dagger(\boldsymbol{k})]/\sqrt{2}$ as

$$H_\uparrow + H_\downarrow = \sum_{\sigma=\pm} \int \frac{d\boldsymbol{k}}{(2\pi)^3} \, \epsilon_{\boldsymbol{k}} \, \psi_{A\sigma}^\dagger(\boldsymbol{k})\psi_{A\sigma}(\boldsymbol{k}) + \sum_{m=-\ell}^{\ell} \delta_m \phi_m^\dagger \phi_m$$
$$+ \sum_{\sigma=\pm} \sum_{m=-\ell}^{\ell} \int \frac{d\boldsymbol{k}}{(2\pi)^3} \left[\frac{V_\ell^m(\boldsymbol{k})}{\sqrt{2}} \psi_{A\sigma}^\dagger(\boldsymbol{k})\psi_B^\dagger \phi_m + \mathrm{H.c.}\right], \qquad (7)$$

where A_- and A_+ atoms equally interact with the impurity B atom. Remarkably, the resulting Hamiltonian is identical to the Anderson impurity model extended to study tunneling of electrons through a quantum dot [7, 8] with roles of left and right leads played by our two superposition states. The chemical potential imbalance $\Delta\mu \neq 0$ thus causes a transport of fermions from majority to minority superposition states through scatterings with the impurity B atom [38]. After a period of Δt, the numbers of A_- and A_+ atoms change into $N_- + I\Delta t$ and $N_+ - I\Delta t$ with I being the steady-state current.

(iii) Measurement: We then turn off the confinement-induced resonance to terminate the transport. By applying the intercomponent coupling (6) again but for a duration of $3\pi/(2\Omega)$, the two superposition states are transformed back into the original two spin components as $|A_-\rangle \to -|A_\uparrow\rangle$ and $|A_+\rangle \to -|A_\downarrow\rangle$ whose numbers are now $N_- + I\Delta t$ and $N_+ - I\Delta t$, respectively. Finally, from the measured numbers of $A_\uparrow$ and $A_\downarrow$ atoms compared to their initial values, the transported fermion number $I\Delta t$ can be extracted to determine the conductance $I/\Delta\mu$ of the transport Hamiltonian (7). This constitutes the ultracold atom equivalent of the conductance measurement in quantum dot systems.

III. CONDUCTANCE AND THE KONDO EFFECT

In order to provide quantitative guides on how the orbital Kondo effect emerges in the proposed conductance measurement with ultracold atoms, we study in detail the linear conductance $G = \lim_{\Delta\mu\to 0} I/\Delta\mu$ of the transport Hamiltonian (7). With the aid of the Meir-Wingreen formula for the steady-state current $I = (dN_-/dt - dN_+/dt)/2$ [39], the linear conductance is given by

$$G = \frac{1}{\hbar} \sum_{m=-\ell}^{\ell} \int \frac{d\boldsymbol{k}}{(2\pi)^3} \frac{|V_\ell^m(\boldsymbol{k})|^2}{2} f_T'(\epsilon_{\boldsymbol{k}} - \mu) \, \mathrm{Im}\, \mathcal{G}_m^R(\epsilon_{\boldsymbol{k}} - \mu),$$

(8)

where $f_T(z) = 1/(e^{\beta z}+1)$ is the Fermi-Dirac distribution function at an inverse temperature $\beta = 1/(k_\mathrm{B}T)$ and

$$\mathcal{G}_m^R(\epsilon) = -\frac{i}{\hbar} \int_0^\infty dt\, e^{i\epsilon t/\hbar} \langle \{\psi_B^\dagger(t)\phi_m(t), \phi_m^\dagger(0)\psi_B(0)\}\rangle$$

(9)

is the retarded Green's function with the expectation value taken with respect to the equilibrium state at $\Delta\mu = 0$. Therefore, A_- and A_+ atoms now have the equal chemical potential $\mu_\pm = \mu$ and thus it is advantageous to express the transport Hamiltonian (7) on the original spin basis so that it is decoupled into Eqs. (1) and (5) [40]. Because $A_\downarrow$ atoms do not interact with the impurity B atom, the expectation value is simply evaluated as $\langle\cdots\rangle = \mathrm{Tr}[e^{-\beta(H_\uparrow - \mu N_\uparrow)}\cdots]/Z$ along with the constraint (3), where

$$N_\uparrow = \int \frac{d\boldsymbol{k}}{(2\pi)^3} \psi_{A\uparrow}^\dagger(\boldsymbol{k})\psi_{A\uparrow}(\boldsymbol{k}) + \sum_{m=-\ell}^{\ell} \phi_m^\dagger \phi_m$$

(10)

is the particle number operator of $A_\uparrow$ atoms. While the equilibrium Green's function (9) can be computed by means of various methods [41], we here employ the so-called noncrossing approximation [2, 42], which is known to be reliable for large degeneracy and not too low temperature, and thus adequate for our purpose.
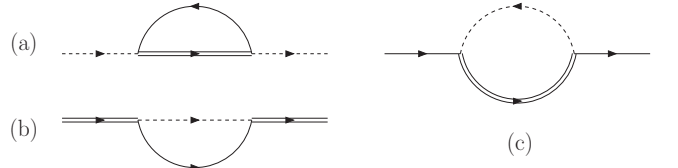

FIG. 1. Noncrossing approximation for self-energies of the localized (a) B atom [Eq. (11)] and (b) bound molecule [Eq. (12)] as well as (c) the Matsubara Green's function corresponding to Eq. (9). Solid, dashed, and doubled lines represent the propagators of $A_\uparrow$ atom, B atom, and bound molecule, respectively.

The propagators of the localized B atom and bound molecule are sometimes called resolvents and denoted by $\mathcal{R}_B(z) = [z - \Sigma_B(z)]^{-1}$ and $\mathcal{R}_m(z) = [z + \mu - \delta_m - \Sigma_m(z)]^{-1}$, respectively. Their self-energies within the noncrossing approximation are depicted in Fig. 1 and determined self-consistently according to

$$\Sigma_B(z) = \sum_{\ell=-m}^{m} \int \frac{d\boldsymbol{k}}{(2\pi)^3} |V_\ell^m(\boldsymbol{k})|^2 f_T(\epsilon_{\boldsymbol{k}} - \mu) \, \mathcal{R}_m(z + \epsilon_{\boldsymbol{k}} - \mu)$$

(11)

and

$$\Sigma_m(z) = \int \frac{d\boldsymbol{k}}{(2\pi)^3} |V_\ell^m(\boldsymbol{k})|^2 f_T(\mu - \epsilon_{\boldsymbol{k}}) \, \mathcal{R}_B(z - \epsilon_{\boldsymbol{k}} + \mu).$$

(12)

In terms of the corresponding spectral densities of $\rho_B(\epsilon) = -(1/\pi)\,\mathrm{Im}\,\mathcal{R}_B(\epsilon + i0^+)$ and $\rho_m(\epsilon) = -(1/\pi)\,\mathrm{Im}\,\mathcal{R}_m(\epsilon + i0^+)$, the imaginary part of the retarded Green's function (9) is expressed as

$$-\frac{1}{\pi}\,\mathrm{Im}\,\mathcal{G}_m^R(\epsilon) = \frac{1 + e^{-\beta\epsilon}}{Z_B} \int_{-\infty}^{\infty} dz\, e^{-\beta z} \rho_B(z)\rho_m(z + \epsilon)$$

(13)

with

$$Z_B = \int_{-\infty}^{\infty} dz\, e^{-\beta z} \left[\rho_B(z) + \sum_{m=-\ell}^{\ell} \rho_m(z)\right]$$

(14)

being the impurity partition function [2, 42]. The substitution of Eq. (13) into Eq. (8) now allows us to compute the linear conductance numerically for a given set of parameters.

Besides the chemical potential μ and temperature T of $A_\uparrow$ atoms, the linear conductance (8) depends on the detuning δ_m and coupling v_m as well as the wave-number cutoff Λ through $V_\ell^m(\boldsymbol{k})$ defined in Eq. (2). In order to make contact with ultracold atom experiments, the bare parameters δ_m and v_m should be expressed in terms of physical parameters such as the scattering length a_m and the resonance range r_m characterizing low-energy scatterings in the ℓth partial-wave channel. They can be related by matching the two-body scattering $\mathcal{T}$ matrix in

the vacuum computed from the two-channel Hamiltonian (1) with the standard form of

$$\mathcal{T}_\ell(k) = \frac{8\pi^2\hbar^2}{M} \sum_{m=-\ell}^{\ell} \frac{k^{2\ell} Y_\ell^m(\hat{\boldsymbol{k}}_{\text{out}})\bar{Y}_\ell^m(\hat{\boldsymbol{k}}_{\text{in}})}{ik^{2\ell+1} + 1/a_m + r_m k^2 + O(k^4)},$$
(15)

where we find

$$\frac{1}{a_m} = -\frac{8\pi^2\hbar^2\delta_m}{Mv_m^2} + \frac{\Gamma(\ell+\frac{1}{2})\Lambda^{2\ell+1}}{\pi}$$
(16)

and

$$r_m = \frac{1}{a_m\Lambda^2} + \frac{4\pi^2\hbar^4}{M^2v_m^2} + \frac{\Gamma(\ell-\frac{1}{2})\Lambda^{2\ell-1}}{\pi}.$$
(17)

In the vicinity of the confinement-induced resonance $1/a_m \ll \Lambda^{2\ell+1}$, the two-body scattering $\mathcal{T}$ matrix (15) has a pole in terms of the scattering energy $\epsilon = \hbar^2k^2/(2M)$ at $\epsilon_m = -\hbar^2/(2Ma_mr_m)$, which is the physical molecular energy and tunable in ultracold atom experiments. These dimensionful quantities are customarily normalized with respect to the Fermi wave number k_{F} defined through the particle number density of $A_\uparrow$ atoms as $k_{\text{F}}^3/(6\pi^2) = \int d\boldsymbol{k}/(2\pi)^3 f_T(\epsilon_{\boldsymbol{k}} - \mu)$. Consequently, the linear conductance (8) is parameterized by $\epsilon_m/\epsilon_{\text{F}}$, $r_m/k_{\text{F}}^{2\ell-1}$, Λ/k_{F}, and T/T_{F} with $\epsilon_{\text{F}} = \hbar^2k_{\text{F}}^2/(2M)$ and $T_{\text{F}} = \epsilon_{\text{F}}/k_{\text{B}}$ being the Fermi energy and temperature, respectively.

While the formulation developed so far is general, we now focus on the confinement-induced p-wave resonance in a dilute system with $\ell = 1$ and $\Lambda = 10k_{\text{F}}$. Figure 2 shows the computed linear conductance G in units of the Planck constant $h = 2\pi\hbar$ in the SU(3) symmetric case with the resonance range $r_m = \Lambda$ chosen corresponding to the case where the confined B atom is lighter than A atoms [34]. In the upper panel, hG is plotted as a function of the threefold degenerate molecular energy $0 \le \epsilon_m/\epsilon_{\text{F}} \le 2$ for selected temperatures $T/T_{\text{F}} = 0.01$, 0.02, 0.05, 0.1, 0.2, 0.5, and 1 accessible in ultracold atom experiments. When the molecular energy is above the Fermi energy ($\epsilon_m \gtrsim \epsilon_{\text{F}}$), the conductance decreases toward the low temperature until it eventually reaches a single Lorentzian curve with its width set by the molecular lifetime. On the other hand, when the molecular energy is below the Fermi energy ($\epsilon_m \lesssim \epsilon_{\text{F}}$), the conductance exhibits a strikingly distinct behavior, i.e., logarithmic growth by lowering the temperature, which is the hallmark of the Kondo effect. Actually, the most remarkable feature of the Kondo effect is the fact that the conductance turns out to be the universal function of the temperature characterized by a single quantity T_{K} in which all microscopic details are encoded [43]. Such universality is demonstrated in the lower panel of Fig. 2 where hG for selected molecular energies $\epsilon_m/\epsilon_{\text{F}} = 0.6$, 0.65, 0.7, 0.75, 0.8, 0.85, and 0.9 are plotted in the same temperature range of $0.01T_{\text{F}} \le T \le T_{\text{F}}$ but normalized individually by $T_{\text{K}} \approx 0.0072T_{\text{F}}$, 0.012$T_{\text{F}}$, 0.019$T_{\text{F}}$,
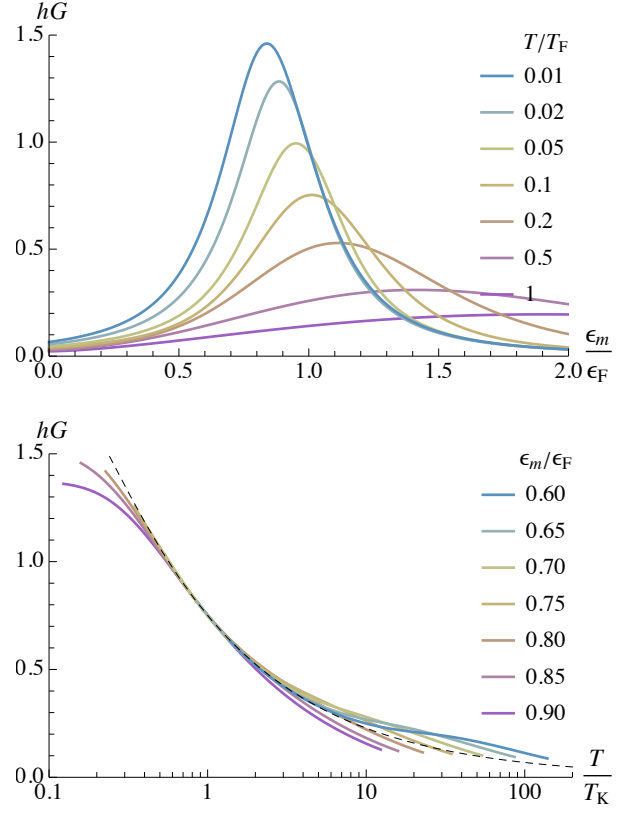

FIG. 2. Linear conductance G in the SU(3) symmetric case with $\ell = 1$, $\Lambda = 10k_{\text{F}}$, and $r_m = \Lambda$ as a function of the threefold degenerate molecular energy $\epsilon_m = -\hbar^2/(2Ma_mr_m)$ for selected $T/T_{\text{F}} = 0.01$, 0.02, 0.05, 0.1, 0.2, 0.5, and 1 from highest to lowest curves (upper panel) and as a function of the temperature T for selected $\epsilon_m/\epsilon_{\text{F}} = 0.6$, 0.65, 0.7, 0.75, 0.8, 0.85, and 0.9 from rightmost to leftmost curves (lower panel). All curves in the lower panel are plotted in the same temperature range of $0.01T_{\text{F}} \le T \le T_{\text{F}}$ but normalized individually by T_{K} for each $\epsilon_m/\epsilon_{\text{F}}$ so as to best fit to a common empirical form (18) of $hG(T) \approx (9/4)/[1+67.(T/T_{\text{K}})^2]^{0.26}$ indicated by the dashed curve.

$0.029T_{\text{F}}$, $0.044T_{\text{F}}$, $0.063T_{\text{F}}$, and $0.081T_{\text{F}}$ so that all curves come together to make up a single universal curve as much as possible. The obtained universal function is found to be well described by the empirical form [44] of

$$G(T) = \frac{G_0}{[1 + (3^{1/\gamma} - 1)(T/T_{\text{K}})^2]^\gamma},$$
(18)

where $G_0 = (2\ell + 1)\sin^2[\pi/(2\ell + 1)]/h$ is the zero temperature conductance for the SU($2\ell+1$) Kondo effect in our realization [45], the Kondo temperature is defined by $G(T_{\text{K}}) = G_0/3$, and the exponent $\gamma \approx 0.26$ is chosen so as to achieve the best fit to the numerical data. While the Kondo temperature decreases exponentially toward the molecular limit $\epsilon_m/\epsilon_{\text{F}} \to -\infty$ as in Eq. (4), we find a reasonable range of molecular energy $0.5 \lesssim \epsilon_m/\epsilon_{\text{F}} \lesssim 1$ where the universal logarithmic growth of the conductance is observable in ultracold atom experiments.
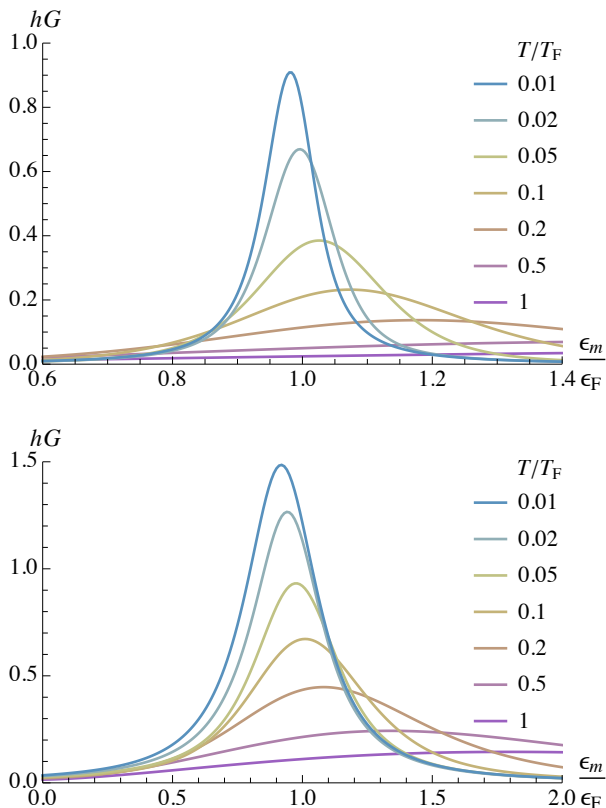
FIG. 3. Same as the upper panel of Fig. 2 with $\ell = 1$ and $\Lambda = 10k_{\mathrm{F}}$ but for a narrower resonance with $r_m = 5\Lambda$ (upper panel) and in a symmetry broken case to SU(2) with twofold degenerate $\epsilon_m = \epsilon_{\pm 1}$ and decoupled $\epsilon_0 \to \infty$ (lower panel).

The linear conductance G as a function of the molecular energy is also computed for different sets of parameters as shown in Fig. 3 with $\ell = 1$ and $\Lambda = 10k_{\mathrm{F}}$ retained. The upper panel is in the SU(3) symmetric case as before but now for the larger resonance range of $r_m = 5\Lambda$ corresponding to the case where the confined B atom is heavier than A atoms [34]. While the Kondo effect is still observable in the plotted temperature range, the Kondo temperature gets lower and the peak structure gets narrower. On the other hand, the lower panel is aimed at elucidating the effect of symmetry breaking by setting the resonance range back to $r_m = \Lambda$. Here we suppose that the isotropic confinement potential acting on the

impurity B atom is strongly deformed to a uniaxial one so that the p-orbital degeneracy is reduced to twofold with $\epsilon_m = \epsilon_{\pm 1}$ and the nondegenerate molecular state is decoupled with its energy $\epsilon_0 \to \infty$. The resulting peak structure of the conductance in the lower panel of Fig. 3 is found to remain almost unchanged from that in the upper panel of Fig. 2 and thus the observability of the Kondo effect is not impaired by the symmetry breaking from SU(3) to SU(2).

IV. CONCLUDING REMARKS

In this Rapid Communication, we proposed and elaborated a simple and versatile scheme to perform the conductance measurement with ultracold atoms by employing spin superposition states, which can be implemented, for example, in a Fermi gas of lithium atoms with impurity ytterbium atoms [46]. In particular, we showed that a confinement-induced p-wave or higher partial-wave resonance leads to the universal logarithmic growth of the conductance toward the low temperature, which is within reach of observation and thus provides a clear evidence of the orbital Kondo effect in ultracold atom experiments. Not only the proposed transport measurement is applicable both in and out of equilibrium, but our system is highly tunable and can be easily extended to a dense Kondo lattice [22], which is difficult to realize in quantum dot systems in spite of its importance to heavy fermion physics. It will be interesting to further incorporate a strong attraction between two components of fermions so that they form Cooper pairs exhibiting the BCS-BEC crossover. The possibility to study such a rich variety of Kondo physics with ultracold atoms is now opened up.

[1] P. W. Anderson, "Localized magnetic states in metals," Phys. Rev. **124**, 41-53 (1961).

[2] A. C. Hewson, *The Kondo Problem to Heavy Fermions* (Cambridge University Press, Cambridge, UK, 1993).

[3] J. Kondo, "Resistance minimum in dilute magnetic alloys," Prog. Theor. Phys. **32**, 37-49 (1964).

[4] J. R. Schrieffer and P. A. Wolff, "Relation between the Anderson and Kondo Hamiltonians," Phys. Rev. **149**, 491-492 (1966).

[5] B. Coqblin and J. R. Schrieffer, "Exchange interaction in alloys with cerium impurities," Phys. Rev. **185**, 847-853 (1969).

[6] P. Coleman, "Heavy fermions: Electrons at the edge of magnetism," in *Handbook of Magnetism and Advanced Magnetic Materials,* edited by H. Kronmüller and S. Parkin (John Wiley & Sons, New York, 2007).

[7] Y. Meir, N. S. Wingreen, and P. A. Lee, "Transport through a strongly interacting electron system: Theory

of periodic conductance oscillations," Phys. Rev. Lett. **66**, 3048-3051 (1991).

[8] Y. Meir, N. S. Wingreen, and P. A. Lee, "Low-temperature transport through a quantum dot: The Anderson model out of equilibrium," Phys. Rev. Lett. **70**, 2601-2604 (1993).

[9] L. I. Glazman and M. E. Raikh, "Resonant Kondo transparency of a barrier with quasilocal impurity states," JETP Lett. **47**, 452-455 (1988).

[10] T. K. Ng and P. A. Lee, "On-site Coulomb repulsion and resonant tunneling," Phys. Rev. Lett. **61**, 1768-1771 (1988).

[11] M. Grobis, I. G. Rau, R. M. Potok, and D. Goldhaber-Gordon, "The Kondo effect in mesoscopic quantum dots," in *Handbook of Magnetism and Advanced Magnetic Materials,* edited by H. Kronmüller and S. Parkin (John Wiley & Sons, New York, 2007).

[12] W. G. van der Wiel and S. De Franceschi, "Kondo effect in quantum dots," in *Handbook of Nanophysics: Nanoparticles and Quantum Dots,* edited by K. D. Sattler (CRC Press, Boca Raton, FL, 2010).

[13] See, for example, M. Lewenstein, A. Sanpera, and V. Ahufinger, *Ultracold Atoms in Optical Lattices: Simulating Quantum Many-Body Systems* (Oxford University Press, Oxford, UK, 2012).

[14] J.-P. Brantut, J. Meineke, D. Stadler, S. Krinner, and T. Esslinger, "Conduction of ultracold fermions through a mesoscopic channel," Science **337**, 1069-1071 (2012).

[15] D. Stadler, S. Krinner, J. Meineke, J.-P. Brantut, and T. Esslinger, "Observing the drop of resistance in the flow of a superfluid Fermi gas," Nature (London) **491**, 736-739 (2012).

[16] S. Krinner, D. Stadler, J. Meineke, J.-P. Brantut, and T. Esslinger, "Superfluidity with disorder in a thin film of quantum gas," Phys. Rev. Lett. **110**, 100601 (2013).

[17] J.-P. Brantut, C. Grenier, J. Meineke, D. Stadler, S. Krinner, C. Kollath, T. Esslinger, and A. Georges, "A thermoelectric heat engine with ultracold atoms," Science **342**, 713-715 (2013).

[18] S. Krinner, D. Stadler, D. Husmann, J.-P. Brantut, and T. Esslinger, "Observation of quantized conductance in neutral matter," Nature (London) **517**, 64-67 (2015).

[19] J. Lee, S. Eckel, F. Jendrezjewski, C. J. Lobb, G. K. Campbell, and W. T. Hill, III, "Contact resistance and phase slips in mesoscopic superfluid atom transport," arXiv:1506.08413 [cond-mat.quant-gas].

[20] D. Husmann, S. Uchino, S. Krinner, M. Lebrat, T. Giamarchi, T. Esslinger, and J.-P. Brantut, "Connecting strongly correlated superfluids by a quantum point contact," Science **350**, 1498-1501 (2015).

[21] L. Kouwenhoven and L. Glazman, "Revival of the Kondo effect," Phys. World **14**, 33-38 (2001).

[22] Y. Nishida, "SU(3) orbital Kondo effect with ultracold atoms," Phys. Rev. Lett. **111**, 135301 (2013).

[23] A. Recati, P. O. Fedichev, W. Zwerger, J. von Delft, and P. Zoller, "Dissipative spin-boson model and Kondo effect in low dimensional quantum gases," arXiv:cond-mat/0212413.

[24] G. M. Falco, R. A. Duine, and H. T. C. Stoof, "Molecular Kondo resonance in atomic Fermi gases," Phys. Rev. Lett. **92**, 140402 (2004).

[25] L.-M. Duan, "Controlling ultracold atoms in multi-band optical lattices for simulation of Kondo physics," Europhys. Lett. **67**, 721-727 (2004).

[26] B. Paredes, C. Tejedor, and J. I. Cirac, "Fermionic atoms in optical superlattices," Phys. Rev. A **71**, 063608 (2005).

[27] A. V. Gorshkov, M. Hermele, V. Gurarie, C. Xu, P. S. Julienne, J. Ye, P. Zoller, E. Demler, M. D. Lukin, and A. M. Rey, "Two-orbital SU(N) magnetism with ultracold alkaline-earth atoms," Nat. Phys. **6**, 289-295 (2010).

[28] S. Lal, S. Gopalakrishnan, and P. M. Goldbart, "Approaching multichannel Kondo physics using correlated bosons: Quantum phases and how to realize them," Phys. Rev. B **81**, 245314 (2010).

[29] J. Bauer, C. Salomon, and E. Demler, "Realizing a Kondo-correlated state with ultracold atoms," Phys. Rev. Lett. **111**, 215304 (2013).

[30] I. Kuzmenko, T. Kuzmenko, Y. Avishai, and K. Kikoin, "Model for overscreened Kondo effect in ultracold Fermi gas," Phys. Rev. B **91**, 165131 (2015).

[31] B. Sundar and E. J. Mueller, "Proposal to directly observe the Kondo effect through enhanced photo-induced scattering of cold fermionic and bosonic atoms," arXiv:1503.05234 [cond-mat.quant-gas].

[32] M. Nakagawa and N. Kawakami, "Laser-induced Kondo effect in ultracold alkaline-earth fermions," Phys. Rev. Lett. **115**, 165303 (2015).

[33] K. R. Patton, "A fully controllable Kondo system: Coupling a flux qubit and an ultracold Fermi gas," arXiv:1508.03016 [cond-mat.quant-gas].

[34] Y. Nishida and S. Tan, "Confinement-induced p-wave resonances from s-wave interactions," Phys. Rev. A **82**, 062713 (2010).

[35] S. E. Barnes, "New method for the Anderson model," J. Phys. F: Met. Phys. **6**, 1375-1383 (1976); "New method for the Anderson model: II. The $U = 0$ limit," J. Phys. F: Met. Phys. **7**, 2637-2647 (1977).

[36] P. Coleman, "New approach to the mixed-valence problem," Phys. Rev. B **29**, 3035-3044 (1984).

[37] M. Knap, A. Shashi, Y. Nishida, A. Imambekov, D. A. Abanin, and E. Demler, "Time-dependent impurity in ultracold fermions: Orthogonality catastrophe and beyond," Phys. Rev. X **2**, 041020 (2012).

[38] Even when the interaction between $A_\uparrow$ and $A_\downarrow$ atoms is non-negligible, it does not cause an undesired bulk transport between the two superposition states, as is evident from its expression of $\int d\boldsymbol{r}\, \psi_{A\uparrow}^\dagger(\boldsymbol{r})\psi_{A\downarrow}^\dagger(\boldsymbol{r})\psi_{A\downarrow}(\boldsymbol{r})\psi_{A\uparrow}(\boldsymbol{r}) = \int d\boldsymbol{r}\, \psi_{A+}^\dagger(\boldsymbol{r})\psi_{A-}^\dagger(\boldsymbol{r})\psi_{A-}(\boldsymbol{r})\psi_{A+}(\boldsymbol{r})$.

[39] Y. Meir and N. S. Wingreen, "Landauer formula for the current through an interacting electron region," Phys. Rev. Lett. **68**, 2512-2515 (1992).

[40] It is worthwhile to note that $A_\uparrow$ and $A_\downarrow$ atoms are not decoupled if $\Delta\mu \neq 0$ because the chemical potential terms are expressed as $\sum_{\sigma=\pm} \mu_\pm \psi_{A\sigma}^\dagger \psi_{A\sigma} = \mu\,(\psi_{A\uparrow}^\dagger \psi_{A\uparrow} + \psi_{A\downarrow}^\dagger \psi_{A\downarrow}) + (\Delta\mu/2)(\psi_{A\uparrow}^\dagger \psi_{A\downarrow} + \psi_{A\downarrow}^\dagger \psi_{A\uparrow})$.

[41] A. Georges, G. Kotliar, W. Krauth, and M. J. Rozenberg, "Dynamical mean-field theory of strongly correlated fermion systems and the limit of infinite dimensions," Rev. Mod. Phys. **68**, 13-125 (1996).

[42] N. E. Bickers, "Review of techniques in the large-N expansion for dilute magnetic alloys," Rev. Mod. Phys. **59**, 845-939 (1987).

[43] T. A. Costi, A. C. Hewson, and V. Zlatić, "Transport coefficients of the Anderson model via the numerical renormalization group," J. Phys. Condens. Matter **6**, 2519-2558 (1994).

[44] D. Goldhaber-Gordon, J. Göres, M. A. Kastner, H. Shtrikman, D. Mahalu, and U. Meirav, "From the Kondo regime to the mixed-valence regime in a single-electron transistor," Phys. Rev. Lett. **81**, 5225-5228 (1998).

[45] A. Carmi, Y. Oreg, and M. Berkooz, "Realization of the SU(N) Kondo effect in a strong magnetic field," Phys. Rev. Lett. **106**, 106401 (2011).

[46] H. Hara, H. Konishi, S. Nakajima, Y. Takasu, and Y. Takahashi, "A three-dimensional optical lattice of ytterbium and lithium atomic gas mixture," J. Phys. Soc. Jpn. **83**, 014003 (2014).